**Journal of Photonic Materials and Technology**
2022; 8(1): 1-10
http://www.sciencepublishinggroup.com/j/jpmt
doi: 10.11648/j.jmpt.20220801.11
ISSN: 2469-8423 (Print); ISSN: 2469-8431 (Online)

# Light Transmission Through One-Dimensional Photonic Crystal Filters for Thermophotovoltaic Applications

**Faustin Hilaire Tchoffo, Fabrice Kwefeu Mbakop*, Jean Luc Dit Bouerdjila Nsouandele, Noel Djongyang**

Department of Renewable Energy, National Advanced School of Engineering, University of Maroua (UMa), Maroua, Cameroon

## Email address:

tchoffus0410@gmail.com (Faustin Hilaire Tchoffo), mbakop.fabrice@gmail.com (Fabrice Kwefeu Mbakop), jlnsouandele @hahoo.fr (Jean Luc Dit Bouerdjila Nsouandele), noeldjongyang@gmail.com (Noel Djongyang)

*Corresponding author

## To cite this article:

Faustin Hilaire Tchoffo, Fabrice Kwefeu Mbakop, Jean Luc Dit Bouerdjila Nsouandele, Noel Djongyang. Light Transmission Through One-Dimensional Photonic Crystal Filters for Thermophotovoltaic Applications. *Journal of Photonic Materials and Technology*. Vol. 8, No. 1, 2022, pp. 1-10. doi: 10.11648/j.jmpt.20220801.11

**Received**: May 19, 2022; **Accepted**: June 17, 2022; **Published**: July 5, 2022

**Abstract:** In this paper, three photonic crystals ($TiO_2/SiO_2$, $TiO_2/MgF_2$, $TiO_2/PbF_2$) one-dimensional (1D-PhCs) with defect layers are designed for possible use as a thermophotovoltaic optical filter (TPV). The temperature of this system is 2000 K. Wien's first law predicts the temperature and permissible wavelengths for TPV systems. It is therefore very important to filter it out of the infrared. The transfer matrix approach (TMM) was used to investigate the influence of the number of periods, the varied short refractive indices (L) of the defect layers, and the angle of incidence on the spectral transmission peak. When the number of layers is varied from 6, 8 and 10, there is an optical improvement in the properties of the spectral filter which tends towards 100% as the number of layers increases. The central wavelength is fixed at 1550nm and allows us to have the peak transmission of light. This transmission is created by a coupling of surface waves. The light does not cross the bandwidth of the crystal when the frequency is in the odd parts and there is a peak transmission of 100%. However, the structure that shows the best match of the transmission peak as the angle varies is the $TiO_2/SiO_2$ structure. Unlike the other structures ($TiO_2/MgF_2$, $TiO_2/PbF_2$) where all the peaks do not reach 100% despite the variations in the angles of incidence and types of polarization. Moreover, in the $TiO_2/SiO_2$ structure all the peaks are at 100% of their transmission whatever the polarization mode and the type of angle chosen.

**Keywords:** Spectral Filter, Photonic Crystals, Transfer Matrix Method, Defect Layers, Thermophotovoltaic

## 1. Introduction

Thermophotovoltaic (TPV) devices directly convert thermal energy into electricity and have uses in waste heat recovery, solar energy collecting, and space applications [1–7]. A TPV system is ecologically friendly and consists of two important key components: an emitter that emits radiation by absorbing incoming photons from the emitter and a TPV cell that may produce electricity by absorbing incident photons from the emitter. The primary difficulties with this approach are low conversion efficiency and power production. By putting the emitter and receiver into close contact, near-field thermal radiation has been proposed for improving TPV power generation [5, 6]. The TPV system, on the other hand, is made up of a thermal radiator (emitter) considered to be a perfect blackbody, a selective filter, and a photovoltaic (PV) cell in contrast to solar photovoltaics, the radiation spectrum absorbed in the PV cells of a TPV system may be tailored to the spectral sensitivity of the PV cells, and losses of useless radiation can be avoided to achieve high efficiency and power production [7, 8]. The PV cell absorbs photons with energies larger than the band gap energy of the cell, resulting in electron hole pairs that may be collected as a current through a linked load [9]. A TPV system's emitter temperature typically varies between 1000 and 2000K. This is optimal for a PV cell with a band gap between 0.5 and 0.75 eV, according to Wien's displacement law. Using GaSb as an example, with a low-direct band gap energy of roughly 0.7 eV, the ideal emitter temperature is around 1600K, corresponding to a wavelength of 1.78 m. This makes it an

excellent choice for a TPV system that converts photon energy into electricity [10-13]. In a TPV system, an ideal filter functions as a perfect high pass filter. It transmits photons with energies greater than the bandgap energy (Rfiltre = 0 for E > Eg i.e. $\lambda < \lambda g$) and reflects back to the emitter photons with energies less than the bandgap energy (Rfiltre = 1 for E < Eg i.e. $\lambda > \lambda g$). The investigation into a TPV system is primarily concerned with increasing its efficiency. The spectrum regulation of heat radiation using a selective filter is an important and practical strategy for this aim. One-dimensional photonic crystals (1D PCs) have the advantage of having a simple structure that is easily fabricated.

Recently, $Si/SiO_2$ photonic crystals were described for dielectric dielectric PCs filters utilized in TPV applications [14-19]. However, the optical performance of several types of metallic-dielectric photonic crystals (MDPCs) has been explored theoretically and/or practically. The transmittance and reflectance of $Ag/SiO_2$ photonic crystals were measured [20-22]. As a result, the existence of fault modes is an essential concern associated to the PBG. When the translation al symmetry in a PC is disrupted, the defect modes are typically to be created. This is accomplished by introducing a defective layer into the PC or deleting a single layer from the structure [23, 24]. In theory, the defect layer works as a cavity, allowing the resonant tunneling mode to occur in the PBG. The existence of defect modes inside the PBG is largely reliant on the PC structure under consideration, including the material and thickness of the defect layer [23–26]. Mbakop et al. [27, 28] investigate the behavior of frequency variation and peak light transmission when the period and angle of incidence vary using a 1D-PhCs $TiO_2/SiO_2$ multi-layer structure. They employ an ideal multilayer structure that conceals the transmission peak and a structure with a faulty layer that reveals the transmission peak.

Figure 1 depicts a schematic representation of the TPV system. The high temperature emitter and GaSb photovoltaic cell are considered to be blackbodies. In front of the GaSb photovoltaic cell is an optical filter.

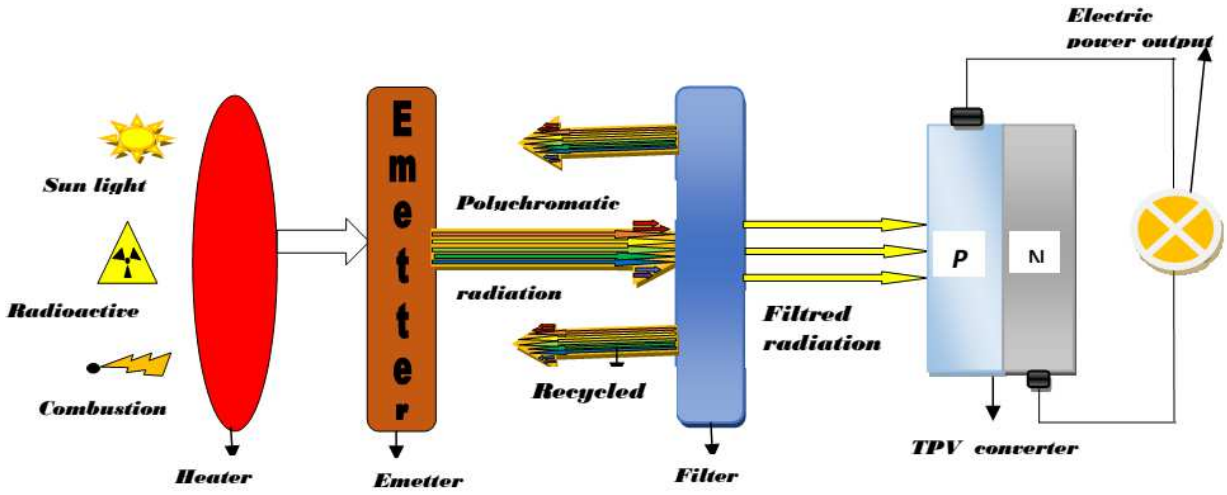


***Figure 1.*** *A general schematic of a TPV system.*

In this study, we propose the design of a one-dimensional photonic crystal filter with a band gap large enough to filter electromagnetic wave radiation. Some electromagnetic wave radiation however, cannot flow through this structure.

## 2. Calculation Method

The transfer matrix method (TMM) [29] will be used to analyze the incident electromagnetic radiation on the structure. The transfer matrix approach is based on the Maxwell equations, which are used to transfer the tangential components of the electric and magnetic field intensity of light from one side of the dielectric layer to the other [30].

We'll make TMM out of the dynamical and propagating matrices that were utilized to represent the wave interaction across each layer and the wave response at the interfaces between them. The boundary conditions for the vectors of the electric field E on each side of an undefined contact may be described simply with a 2x2 matrix [29, 30].

The amplitudes of the plane waves at different layers can be related by.

$$\begin{pmatrix} A_m \\ B_m \end{pmatrix} = D_m^{-1} D_{m+1} P_{m+1} \begin{pmatrix} A_{m+1} \\ B_{m+1} \end{pmatrix} \quad (1)$$

With $m$ = 0, 1, 2,…2N. Where matrices $D$ (dynamical matrix) and $P$ (propagation matrix) can be written as:

$$D_m \begin{pmatrix} 1 & 1 \\ n_m \cos\theta_m & -n_m \cos\theta_m \end{pmatrix} for\ TE\ waves \quad (2)$$

$$D_m \begin{pmatrix} \cos\theta_m & \cos\theta_m \\ n_m & -n_m \end{pmatrix} for\ TM\ waves \quad (3)$$

Since the propagation matrix can be written in the form of sine and cosine functions instead of the exponential function for simplifying [28, 29].

$$P_m = \begin{pmatrix} \cos\emptyset_k + i\sin\emptyset_k & 0 \\ 0 & \cos\emptyset_k - i\sin\emptyset_k \end{pmatrix} \quad (4)$$

$$where\ \emptyset_k = \frac{2\pi d_k}{\lambda} n_k \cos\theta_k, (k = 1, 2, 3 \ldots) \quad (5)$$

Total transfer matrix $M$ for the entire structure given by:

$$M(N_e) = \begin{bmatrix} M_{11} & M_{12} \\ M_{21} & M_{22} \end{bmatrix} = D_0^{-1} M_e^N D_0. \quad (6)$$

Where N is the number of the periods and *Me* is the transfer matrix of one period given by:

$$M_e = D_1 P_1 D_1^{-1} D_2 P_2 D_2^{-1} \quad (7)$$

Then by using the above expressions we can obtain the reflection and the transmission coefficients [30]:

$$r = \frac{M_{21}}{M_{11}}, and\ t = \frac{1}{M_{11}}. \quad (8)$$

### *2.1. Spectral Distribution of the Thermal Transmitter*

Because it completely absorbs all radiation it receives from the heat source, the thermal transmitter operates as a black body. The varied PhC structures must have correspondences with the spectrum distribution of the transmitter at high temperature in the corresponding band of the reflexion and transmission to optimize the one-dimensional filter's reflexion and spectral transmission [18, 19]. The spectral power of a source's radiation at high temperature, according to Planck's law, is given by:

$$E_{(\lambda,T)} = \frac{2\pi hc^2}{\lambda^5\left(exp\left(\frac{hc}{\lambda KT}\right)-1\right)} \quad (9)$$

Where h is the Planck's constant, K the Boltzmann constant and C the speed of the light in the vacuum. The law of Stefan says to us that the total power radiated by a body is:

$$P = \sigma T^4 \quad (10)$$

The wavelength (λm) of the maximum of radiated energy depends on the temperature T following the law known as of the displacement of Wien.

$$\lambda_m T = 2898\ \mu mK \quad (11)$$

### *2.2. Proposed Structure*

The proposed structures consist of one-dimensional photonic crystals $TiO_2/CaF_2$, $Si/CaF_2$ and $Te/CaF_2$ deposited on a quartz substrate. A 1D PhC does not exhibit a complete photonic band gap. However, when coupled to free space it does exhibit total omni-directional reflectance, which can be utilized in TPV systems to improve system performance [23, 24]. The central wavelength of the normal-incidence stop-band can be expressed as:

$$\lambda_0 = \frac{1}{1-\frac{2}{\pi}\sin^{-1}\left(\frac{n_H - n_L}{n_H + n_L}\right)} \lambda_g \quad (12)$$

Where $\lambda_g$ is the normal incidence band gap edge (1.78μm for GaSb cell), $n_H$ and $n_L$ are respectively the refractive indices of the high index (H) and low index (L) layers.

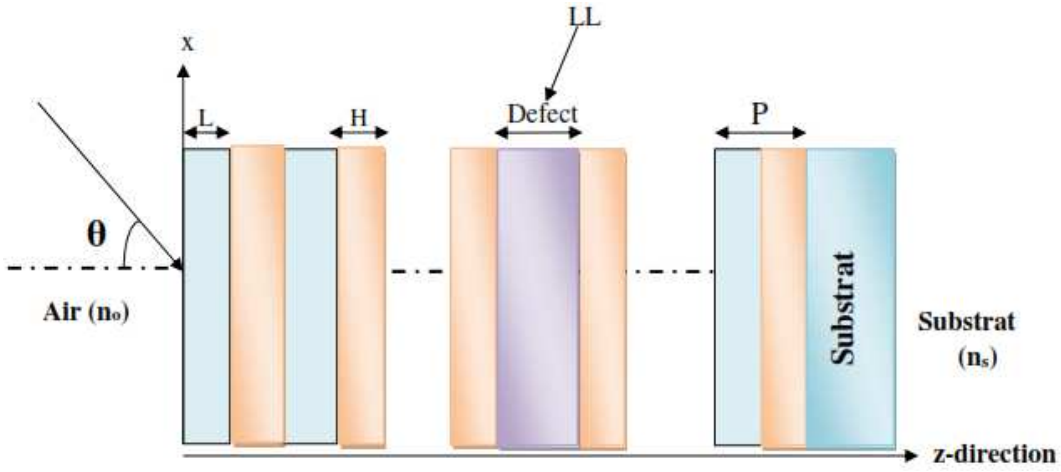


***Figure 2.*** *TPV system with a dielectric filter (1D PhC) deposited on quartz substrate of a layer defect.*

These refractive indices and layer thicknesses are fundamental, as they directly govern the one-dimensional photonic crystal's band gap [19]. The center wavelength of a one-dimensional photonic crystal's photonic band gap should satisfy the following relation:

$$n_L l_L + n_H l_H = \frac{\lambda_0}{2} \quad (13)$$

Where $n_{MgF2}$ and $n_{Si}$ are the refractive indices, $l_{MgF2}$ and $l_{Si}$ are the thicknesses of the first and the second dielectric layers, respectively and $\lambda_0$ is the center wavelength of photonic band gap. In order to have large band gap we use the following relation:

$$n_L l_L = n_H l_H = \frac{\lambda_0}{4} \quad (14)$$

## 3. Results and Discussion

As presented above, the wavelength of the radiation is between 1200 nm and 2200 nm for the study of the spectral

properties and from 1100nm to 200nm for the variation of the angle of incidence. So we need to design a one-dimensional photonic crystal based filter such that its bandgap is between 1200nm and 2200nm. The central wavelength is at 1550 nm corresponding to the wavelength in optical communication. The number of periods is 10, that is to say that we have in total 20 layers composed of 10 layers for materials with large refractive indices (H) composed only of $TiO_2$ (2.4) and 10 layers for materials with low refractive indices (L) composed of $MgF_2$ (1.38), $SiO_2$ (1.46) and $PbF_2$ (1.73). The behavior of the filter for each structure ($TiO_2$ / $MgF_2$, $TiO_2$ / $SiO_2$ and $TiO_2$ / $PbF_2$) will depend on the contrast of the refractive index ($n_H/n_L$) as well as the defect layer at different period.

### *3.1. Behavior of the Temperature of the Emitter*

One of the important problems in improving the spectral transmission performance of a 1D-PhC filter is to properly match the structure of the filter with the spectral distribution of the high temperature transmitter in the corresponding transmission band. For ease of analysis, the emitter is defined as a black body [30-33]. The results corresponding to the wavelength range below 2.0 m are given in Figure 3.

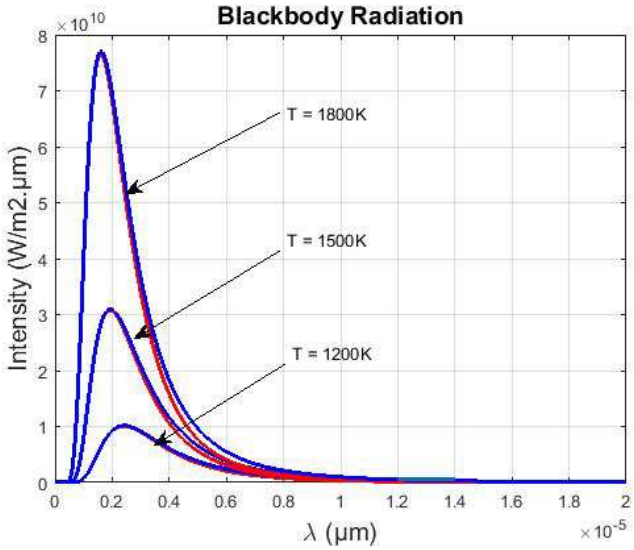


***Figures 3.*** *Spectral radiance of the black body under various temperatures.*

Most of the radiating power of a transmitter was limited in the spectral range of 0 to 2 m. As a result, the filter should be designed in such a way that this wavelength range is in its high transmission band. The amount of light available to a GaSb cell is depicted in Figure 3. The fraction of photons in the spectrum that are above the energy band gap is indicated by the red lines in the figure. We make a variation of the temperature going from 1200K, 1500K to 1800K we observe a clear increase in the intensity of the emittance.

### *3.2. Transmission Spectrum of the Designed Filter*

The Figure 4 represents the transmission curves for a filter without layer defect and with a layer defect.

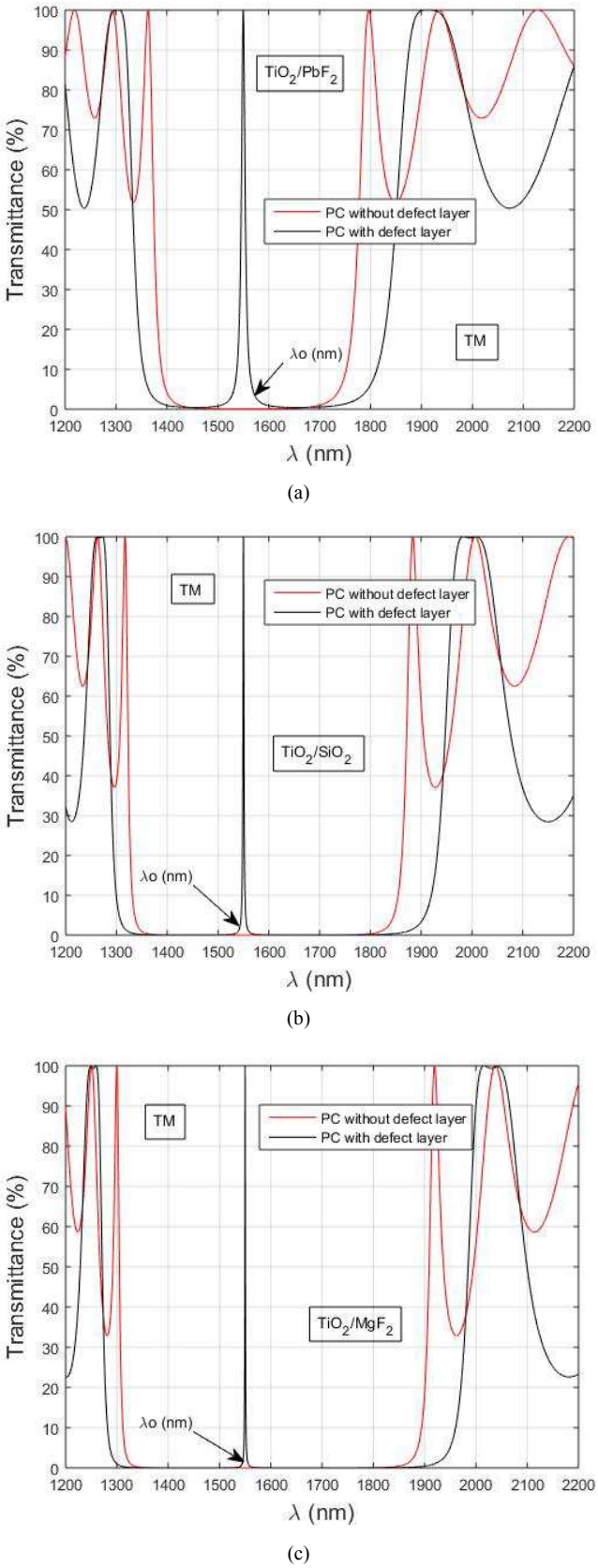


***Figure 4.*** *(a), (b), (c) represent the different structures of TPV filters ($TiO_2/MgF_2$, $TiO_2/PbF_2$, $TiO_2/SiO_2$) each comprising a transmission spectrum of photons without layer defect and another transmission spectrum of photons with layer defect.*

As can be seen in Figures 4(a), (b) and (c), the normal transmittances of structures without fault layer (red) and with fault layer (black) are obtained by the TMM method for TM waves at a period fixed at P = 6. The band gap is in the desired range and all infrared radiation in the area will be reflected by it. The central wavelength also desired is effectively set at 1550 nm. For the case of the default layer, a transmission peak of 100% appears in the gap at λo = 1550 nm. In this case, the resonance at transmission is ensured by the excitation of surface waves at the interface of the film of the photonic crystal.

However, for all of these photonic crystal filters, the structure having a defect layer has a larger band gap than that having no defect layer. In Figure 4(a), we observe that the band gap of the two structures of the $TiO_2/PbF_2$ filter are reduced. The transmission peak is around the center wavelength. Its band gap is equivalent to $\Delta\lambda = 300$nm and its opening wavelength $\lambda_1 = 1400$nm and closing $\lambda_2 = 1700$nm.

For Figure 4(b), of the $TiO_2/SiO_2$ photonic crystal filter, the band gaps of the different structures are significantly larger than those of the structures of the $TiO_2/PbF_2$ filter. However, it is also observed that the pass band represents the asymptotic width of the transmission band and is $\Delta\lambda = 500$nm for an opening wavelength of $\lambda_1 = 1350$nm and a closing wavelength of $\lambda_2 = 1850$nm.

Finally, for Figure 4(c) of the $TiO_2/MgF_2$ photonic crystal filter, we notice that it has a larger band gap than those of the other two filters. It's because of the difference in refractive index ($n_H/n_L$) which is higher. The transmission peak of this filter is exactly centralized on the central wavelength. Therefore, its band gap has a value of $\Delta\lambda = 600$nm having the opening wavelength $\lambda_1 = 1300$nm and the closing wavelength $\lambda_2 = 1900$nm.

Furthermore, the TPV $TiO_2/MgF_2$ and $TiO_2/SiO_2$ photonic crystal filters can be subjected to a higher temperature than that of the $TiO_2/PbF_2$ filter at the same fixed period (P). This is due to the fact that their wavelengths of apertures are located at shorter wavelengths, i.e towards large temperatures according to Wien's laws of displacement. Furthermore, the structure having a defect layer is that which was used to determine the band gaps as well as the wavelengths of openings and closures.

Table 1 shows the values of the different opening and closing wavelengths as well as the band spaces for each TPV filters.

***Table 1.*** *Values of the different band gaps for each TPV filter.*

| Filters TPV | $\lambda_1$ (nm) | $\lambda_2$ (nm) | $\Delta\lambda$ (nm) |
|---|---|---|---|
| $TiO_2/PbF_2$ | 1400 | 1700 | 300 |
| $TiO_2/SiO_2$ | 1350 | 1850 | 500 |
| $TiO_2/MgF_2$ | 1300 | 1900 | 600 |

### *3.3. Effect of Number of Periods on Defect Mode Transmittance for Different Structures*

The Figure 5 shows the transmission peaks of different structures when the number of periods is varied.

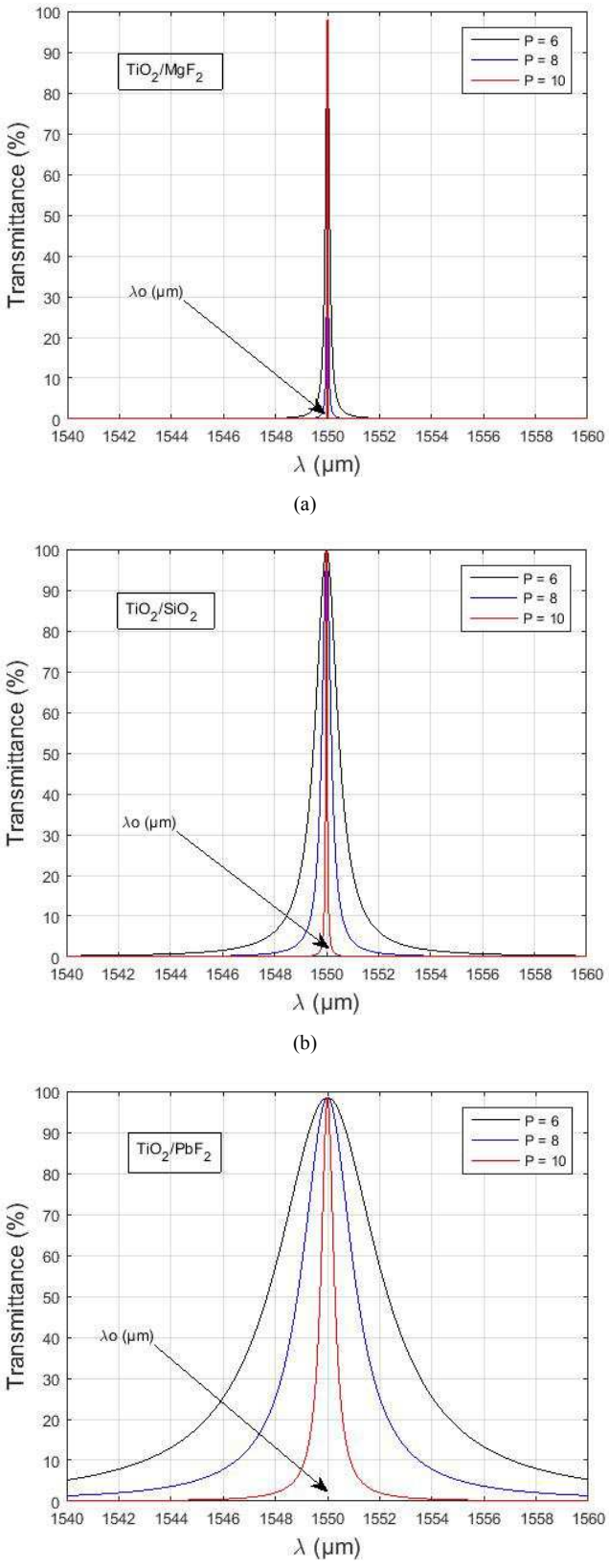


***Figure 5.*** *(a), (b) and (c) represent the different variations of the number of periods on each structure. The different results were obtained using the TMM method for TM waves.*

The stimulation of surface waves at the interface of the

photonic crystal layer ensures resonance at transmission. When the number of pairs of layers grows by P = 6, P = 8, and P = 10, the results of the varied spectrum of the figures above reveal that. However, we observe that the band gap of the fault mode narrows with the increase. The number of periods and the edges of the forbidden band become sharper, which is consistent with the results reported by Mbakop [7]. Furthermore, because the real reflectivity of the mirror is dependent on the refractive index of the cavity medium, this can be explained; i.e. the reflectivity of a quarter-wave stack depends on the refractive index of the medium where the beam is launched and creates a high index medium. When the number of periods is increased from 6 to 10, the full width at half height of the fault mode does not change for the $TiO_2$ /$PbF_2$ structure (Figure 5(a)) but decreases from 2nm to 1nm for the structure $TiO_2$/$SiO_2$ (Figure 5(b)) and from 6nm to 2nm for the $TiO_2$/$MgF_2$ structure (Figure 5(c)) which is consistent with the results reported by Hao et al [34]. By changing the period number of the PC, the band gaps of the default mode can be adjusted. However, we use this concept of peak transmission of structures made of photonic crystals to see the behavior of spectral filters for TPV systems. The Table 1 represents the transmission values for the different structures studied.

***Table 2.*** *Representation of the transmission values for the different structures.*

| Structures | Periods | Transmittance (%) |
|---|---|---|
| | 6 | 98 |
| $TiO_2$/$PbF_2$ | 8 | 98 |
| | 10 | 99 |
| | 6 | 100 |
| $TiO_2$/$SiO_2$ | 8 | 100 |
| | 10 | 100 |
| | 6 | 98 |
| $TiO_2$/$MgF_2$ | 8 | 99 |
| | 10 | 100 |

The $TiO_2$/$SiO_2$ structure exhibits the best transmittance among the structures when the period value is set at P = 10.

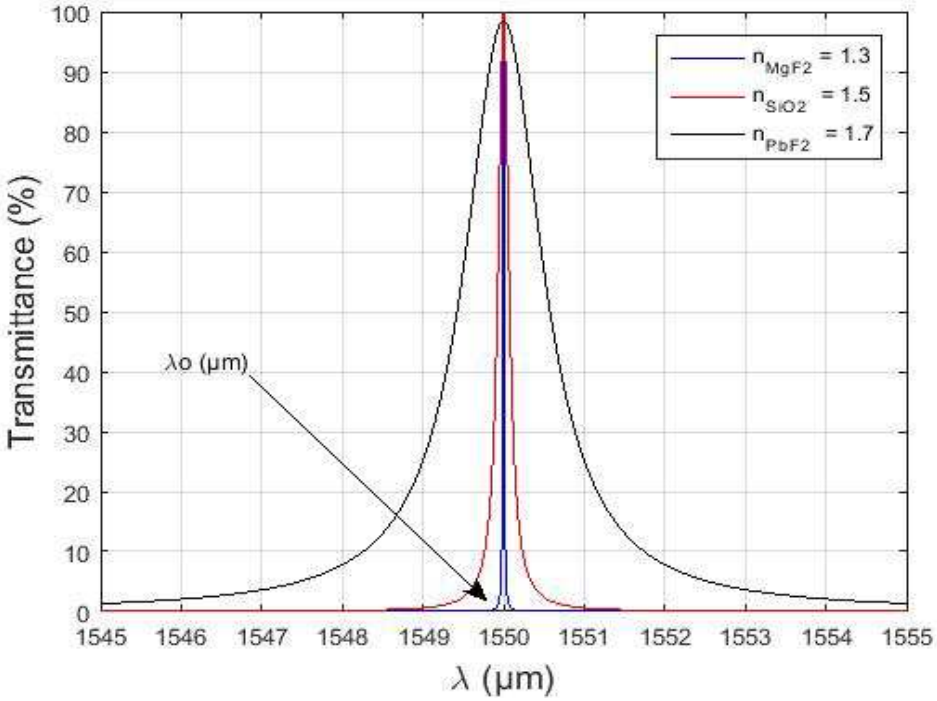


***Figure 6.*** *Representation of the variation of the transmission peaks from the various refractive indices of the defect layer.*

### *3.4. Effect of the Different Short Refractive Index (L) on the Defect Layers*

It is observed in Figure 6 the variation of the transmission peaks of the fault mode from the different refractive indices. Therefore, the thickness of the defect layer must satisfy $n_L l_L = \lambda_o/4$. However, as the refractive index increases, the transmittance of the defective mode decreases. Furthermore, when $n_{MgF_2} = 1.3$, the transmittance is 99.85%, for $n_{S_2O_2} = 1{,}5$, a transmittance of 98% is obtained; while when $n_{P_bF_2} = 1{,}7$, the transmittance decreases to 96% these results are consistent with those obtained by Hao et al [34]. Table 2 represents the different transmittance values.

***Table 3.*** *Variation of the transmission peaks from the various refractive indices of the defect layer.*

| | Refractive index | Transmittance |
|---|---|---|
| $n_{MgF_2}$ | 1.3 | 99.85% |
| $n_{SiO_2}$ | 1.5 | 98% |
| $n_{PbF_2}$ | 1.7 | 96% |

### *3.5. Effect of the Incidence Angle of the Defect Layers on the Transmittance*

The Figure 7 shows the behavior of the transmission peak of the different structures when the angle of incidence is varied.

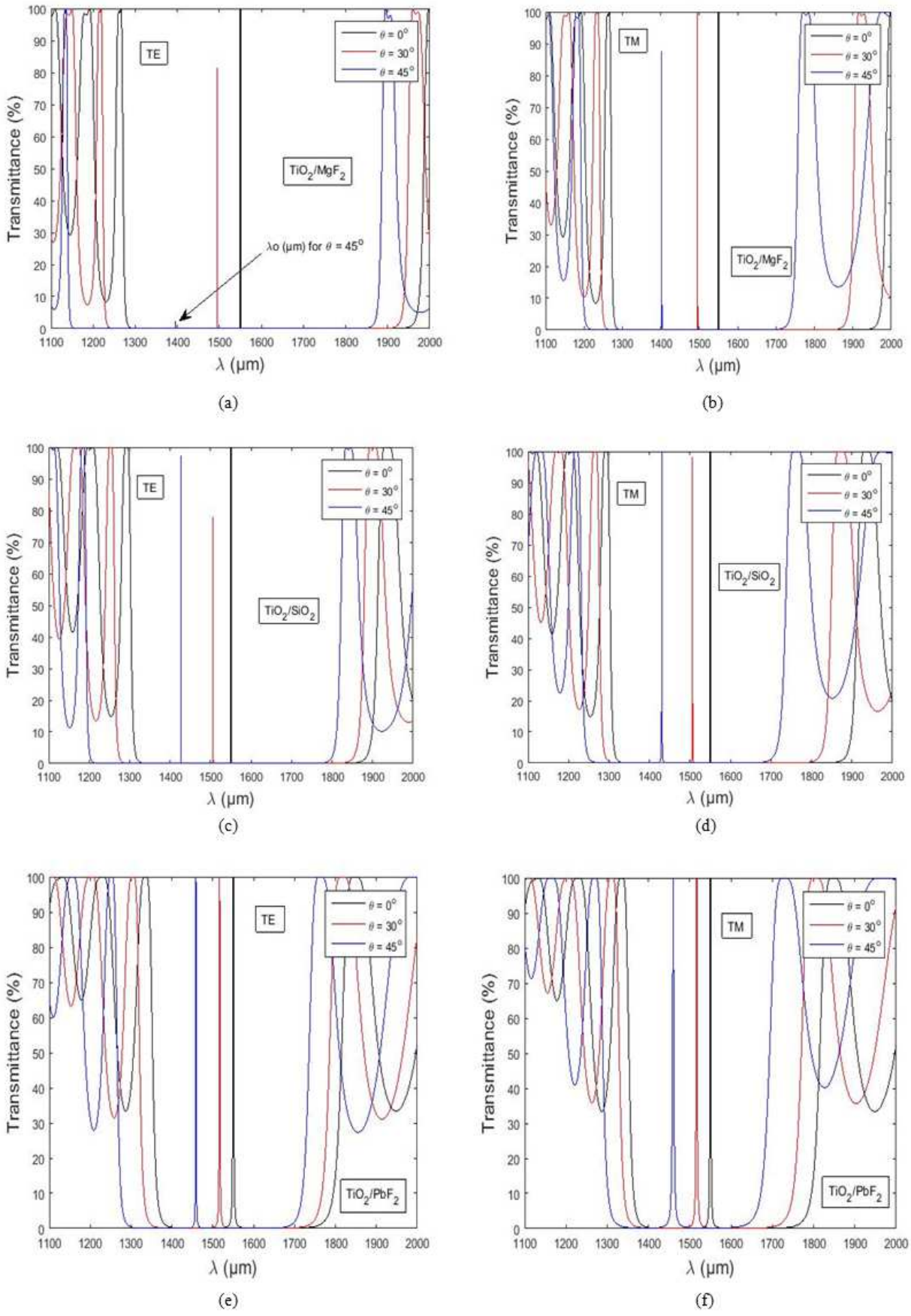


***Figure 7.*** *Variation of the spectral transmittance of the wave for different angles of incidence for the structure exhibiting a layer of defects.*

***Table 4.*** *Shows the values of the transmission peak for different angles of incidence and different values of bandwidth.*

| Structures | Incident angle θ (degree) | TE Polarization | | | TM Polarization | | |
|---|---|---|---|---|---|---|---|
| | | Peak (%) | Transmission Range (nm) | Bandwidth Δλ (nm) | Peak (%) | Transmission Range (nm) | Bandwidth Δλ (nm) |
| $TiO_2/MgF_2$ | 0 | 100 | 1280-1950 | 670 | 100 | 1280-1960 | 680 |
| | 30 | 80 | 1250-1910 | 680 | 100 | 1260-1880 | 620 |
| | 45 | 3 | 1150-1850 | 700 | 85 | 1210-1710 | 500 |
| $TiO_2/SiO_2$ | 0 | 100 | 1320-1880 | 560 | 100 | 1320-1870 | 550 |
| | 30 | 75 | 1280-1850 | 570 | 97 | 1300-1800 | 500 |
| | 45 | 95 | 1200-1800 | 600 | 100 | 1250-1700 | 450 |
| $TiO_2/PbF_2$ | 0 | 100 | 1400-1750 | 350 | 100 | 1400-1750 | 350 |
| | 30 | 100 | 1350-1720 | 370 | 100 | 1380-1700 | 320 |
| | 45 | 100 | 1300-1690 | 390 | 100 | 1350-1630 | 280 |

Figure 7(a), (b), (c), (d), (e), (f) illustrate the transmission spectral of the various structures (including TE and TM polarizations). For the investigation, we used P = 10 period values. The angles of incidence used here are 0°, 30°, and 45°, respectively. However, for the incident wave, we report the results of two polarizations, TE and TM. When the wave is polarized at normal incidence, the TE and TM modes have a same bandgap and transmission peak in all structures. As a result, for all structures, the transmission peak stays centered on the wavelength of 1550 nm. This is in line with the findings of Mbakop et al [7]. However, for the $TiO_2/MgF_2$ structure shown in Figure 7(a), (b), it is observed that the angle of incidence increases up to 30°. There is a difference between TE mode and TM mode. It can be seen that the transmission peak moves rapidly towards the smallest wavelengths (λg = 500nm). Therefore, the bandwidth is equivalent to $\Delta\lambda = \lambda_2 - \lambda_1$ = 680nm. On the other hand, in TM polarization mode the movement is progressive and the transmission peak is equal to 100%. The wavelength remains unchanged as that of the TE mode with a bandwidth of Δλ = 620nm. For a variation of the angle of incidence of 45° in TE mode, the transmission peak is 3% and again moves towards short wavelengths (1400nm). The bandwidth is equal to λg = 700nm. However, in TM mode the transmission peak decreases to 85% for a wavelength of 1400nm. Its bandwidth has a value of Δλ = 500nm.

Figure 7(c), (d), represents the $TiO_2/SiO_2$ structure. We observe the same phenomenon as that of the previous structure. In TE polarization mode for an incidence of 30°, the transmission peak reaches 75% and also shifts to a short wavelength (1510nm). Its bandwidth is equivalent to λg = 570nm. For the same incidence value in TM mode, the transmission peak increases up to a value of 97% for a bandwidth of Δλ = 500nm.

However, when the angle of incidence is varied to 45°, the transmission peak goes from 75% to 95% in TE polarization mode and goes from the central wavelength λg = 1550nm to λg = 1430nm. The bandwidth has a value of Δλ = 600nm. On the other hand, in TM polarization, the peak goes from 97% to 100% for a bandwidth of Δλ=450nm.

Figure 7(e), (f), shows the behavior of the angle of incidence on the $TiO_2/PgF_2$ structure. We observe in this Figure that in TE polarization mode as in TM polarization mode, the different transmission peaks do not change despite the variations in the angle of incidence (0°, 30°, 45°). These transmission peaks shift to short wavelengths as the angle of incidence increases and all have a value of 100%. However, in TE mode when the angle of incidence is fixed at 30° the wavelength changes from 1550nm to 1520nm having a bandwidth of Δλ=370nm for a wavelength of λg=1450nm.

When this angle changes from 30° to 45°, the wavelength remains unchanged and its bandwidth increases Δλ=390nm. On the other hand, in TM mode the movement is also progressive, for an angle of 30° the bandwidth is equivalent to Δλ=20nm. For an angle of 45° the bandwidth decreases and reaches Δλ=280nm for a wavelength of λg=1450nm.

In Figure 7, it is observed that for the three structures, the passband in the TE polarization mode is greater than that in the TM polarization mode. However, the one with the best transmission peak is the $TiO_2/PgF_2$ structure. Unlike the other two, all the peaks of this structure reach a peak of 100% whatever the polarization mode and the type of incidence.

Thus, the peaks of light transmissions of the different structures during the variation of the angles of incidence also make it possible to observe the yields for each angle chosen.

# 4. Conclusion

We explored different one-dimensional photonic crystals 1D ($TiO_2/MgF_2$, $TiO_2/PbF_2$, $TiO_2/SiO_2$ PhC) for the design and construction of spectrally selective filters with a defect layer for use in TPV applications in this paper. The matrix transfer method (TMM) was used in this work for the calculation and development of the influence of the transmission peak of structures with defect layers (LL). This method (TMM) also allowed us to analyze the impact of the period on the transmission peak and the different short refractive indices (L) of the defect layers. In the two polarization modes TM and TE, the influence of the angle of incidence of the different structures on the transmittance was also investigated. Furthermore, when the angle of incidence increases, the transmission band gap decreases and shifts to shorter wavelengths. The center wavelength is set at 1550nm, allowing for maximum light transmission. A coupling of surface waves causes this transmission. When the frequency is in the odd sections of the spectrum and there is a 100 percent transmission peak, light does not flow across the crystal's bandwidth. However, the structure exhibiting the best match in peak transmission as the angle varies is the $TiO_2/SiO_2$ structure. Unlike other structures ($TiO_2/MgF_2$, $TiO_2/PbF_2$) where not all peaks reach 100% despite variations in incidence angles and types of polarization. Furthermore, in the $TiO_2/SiO_2$ structure all the peaks are at

100% of their transmission whatever the polarization mode and the type of angle chosen.

## Acknowledgements

Authors would like to express their deepest and sincere thanks to all the staff of the Renewable Energy Lab of the University of Maroua for their continuous guidance and support during this work.

## References

[1] B. Zhao, L. Wang, Y. Shuai and Z. M. Zhang, (2013) *Thermophotovoltaic emitters based on a two- dimensional grating/thin-film nanostructure,* International Journal of Heat and Mass Transfer 67 637–645.

[2] S. Basu, Y.-B. Chen and Z. M. Zhang (2007) Microscale radiation in thermophotovoltaic devices—a *review*, Int. J. Energy Res. 31 689–716.

[3] T. J. Coutts, (1999) A review of progress in thermophotovoltaic generation of electricity, Renewable Sustainable Energy Rev. 3 77–184.

[4] V. L. Teofilo, P. Choong, J. Chang, Y. L. Tseng and S. Ermer, *(*2008) *Thermophotovoltaic energy conversion for space*, J. Phys Chem. C 112, 7841–7845.

[5] K. Park, S. Basu, W. P. King and Z. M. Zhang, (2008) *Performance analysis of near-field* thermophotovoltaic devices considering absorption distribution, J. Quant. Spectrosc. Radiat. Transfer 109, 305–316.

[6] M. Francoeur, R. Vaillon and M. P. Mengüç, (2011) *Thermal impacts on the performance of* nanoscale-gap thermophotovoltaic power generators, IEEE Trans. Energy Convers. 26, 686–698.

[7] F. Kwefeu Mbakop, A. Tom, A. Dadjé, C. V. Aloyem Kazé and N. Djongyang, (2020) *One-* dimensional comparison of $TiO_2/SiO_2$ and $Si/SiO_2$ photonic crystals filters for thermophotovoltaic applications in visible and infrared, Chinese Journal of Physics 67, 124–134.

[8] V. Badescu. (2001), Thermodynamic theory of thermophotovoltaic solar energy conversion. Journal of Applied Physics; 90: 6476e86.

[9] M. Zenker, A. Heinzel, G. Stollwerck, J. Ferber and J. Luther (2001), *Efficiency and power* density potential of combustion-driven thermophotovoltaic systems using GaSb *photovoltaic cells*. Electron Devices, IEEE Transactions; 48: 367e76.

[10] G. Samah Babiker, S. Yong, O. M. Sid-Ahmed and X. Ming (2014), *One-Dimensional* Multilayer Microstructure Emitter for Thermophotovoltaic Applications, International Journal of Energy, Information and Communications Vol. 5, pp. 9-20.

[11] N. Z. Jovanovic, (2005) Two-Dimension Photonic Crystals as Selective Emitters for Thermophotovoltaic Power Conversion Applications, Thesis, Massachusetts Institute of Technology.

[12] C. Q. Zhang, (2000) Recent progress in high-temperature solar selective coatings, Solar Energy Materials and Solar Cells, vol. 62, no. 1-2, pp. 63-74.

[13] K. Sharma, H. S. Zaidi, C. P. Logofatu and J. R. S. Breuck, (2002) *Optical and* electrical properties of nanostructured metal-silicon-metal photodetectors, IEEE Journal of Quantum Electronics, vol. 38, no. 12, pp. 1651–1660.

[14] Samia Mostafa, H. Nadia Rafat, and A. Sahar El-Naggar. (2012), *One-dimensional* metallic-dielectric ($Ag/SiO_2$) photonic crystals filter for thermophotovoltaic applications Renewable Energy 45 (2012) 245e250.

[15] F. O'Sullivan, I. Celanovic, N. Jovanovic, J. Kassakian, S. Akiyama and K. Wada, (2005) Optical characteristics of one-dimensional $Si/SiO_2$ photonic crystals for *thermophotovoltaic applications* Journal of Applied Physics 97: 033529.

[16] L. Mao, H. Ye (2010), New development of one-dimensional $Si/SiO_2$ photonic crystals filter for thermophotovoltaic applications". Renewable Energy; 35: 249e56.

[17] Celanovic, F. O'Sullivan, M. Ilak, J. Kassakian and D. Perreault (2004), *Design and* optimization of one-dimensional photonic crystals for thermophotovoltaic applications. Optics Letters; 29: 863e5.

[18] L. Guang Ping, X. Yi Min, H. Yu Ge and L. Qiang (2008) *Investigation of one-dimensional* $Si/SiO_2$ photonic crystals for thermophotovoltaic filter. Science in China Series E: Technological Sciences; 51: 2031e9.

[19] Y. Xuan, X. Chen and Y. Han (2011), Design and analysis of solar thermophotovoltaic *systems* Renewable Energy; 36: 374e87.

[20] Y. K Choi, Y. K Ha, J. E. Kim, H. Y. Park and K. Kim (2003), *Improved transmittance in one* dimensional metallic photonic crystals, Physica B: Condensed Matter; 338: 132e5.

[21] N. H. Rafat, S. A. E. l-Naggar and S. I. Mostafa, (2011), *Modeling of a wide band pass optical* filter based on 1D ternary dielectric-metallic-dielectric photonic crystals, Journal of Optics A: Pure and Applied Optics; 13: 085101.

[22] F. K. Mbakop, N. Djongyang, J. Y. Effa, D. Raïdandi, J L. D. B. Nsouandélé and R. Tchinda (2014), Assessment of the radiative properties of some semi-conductors for applications in thermophotovoltaic and thermophotonic conversion systems, International Journal of Basic and Applied Sciences, 3 (4) 401-413.

[23] J. Zaghdoudi and M. Kanzari (2018), One-dimensional photonic crystal filter using a gradient-index layer, Optik 160; 189–196.

[24] S. G. Johnson, M. L. Povinelli and J. D. Joannopoulos (2001), *New photonic-crystal system for integrated optics*, in: Proceedings of SPIE, pp. 4532.

[25] S. G. Moiseev and V. A. Ostatochnikov, (2016), *Defect modes of one-dimensional photonic*-crystal structure with a resonance nanocomposite layer, Quantum. Electron. 46, 743.

[26] J. D. Witmer, J. T. Hill, and A. H. Safavi-Naeini, (2016), *Design of nanobeam photonic crystal* resonators for a silicon-on-lithium-niobate platform, Opt. Express 24; 5876.

[27] F. K. Mbakop, N. Djongyang, G. W. Ejuh, D. Raïdandi, P. Woafo, (2017) Transmission of light through an optical filter of a one-dimensional photonic crystal: application to the solar thermophotovoltaic system, j.physb.2017.04.033.

[28] P. Yeh, (1988) *Optical Waves in Layered Media,* " John Wiley and Sons, New York.

[29] H. A. Arafa, E. A. Rahman and H. S. Hanafey, (2011) *Numerical Studies on Electromagnetic* Waves Properties in Metallic-Dielectric Photonic Crystal, J. Electromag. Anal. Applic., 3, 465-470.

[30] Y. Lin and H. Xu, (2013) Research in light transmission characteristics of one-dimensional photonic crystal, Optik 123.

[31] F. K. Mbakop, N. Djongyang and D. Raïdandi, (2016) *One–dimensional* $TiO_2/SiO_2$ *photonic* crystal filter for thermophotovoltaic applications, J. Euro. Opt. Soc-Rapid. Pub., Springer.

[32] C. Petcu, (2012) The Optical Transmission of One-Dimensional Photonic Crystals *Containing Double-Negative Materials*, National Research and Development Institute for Gas Turbines Bucharest. Romania.

[33] Liu G. P, Xuan Y. M, Han Y. G and Qiang L. I, (2008) *Investigation of one-dimensional* $Si/SiO_2$ photonic crystals for thermophotovoltaic filter, Science in China Series E: Technological Sciences. Springer.

[34] Hao, Kaizi, Li, Zhuo, Wang, Xin, Yang, Suhui, Zhang and Jinying, (2020) *Transmission* characteristics of onedimensional photonic crystal with dielectric defect layer in near-*infrared band*, Proc. SPIE 11564, AOPC.